

University of Groningen

Thickness scaling of ferroelastic domains in PbTiO₃ films on DyScO₃

Nesterov, O.; Matzen, S.; Magen, C.; Vlooswijk, A. H. G.; Catalan, G.; Noheda, B.

Published in:
Applied Physics Letters

DOI:
[10.1063/1.4823536](https://doi.org/10.1063/1.4823536)

IMPORTANT NOTE: You are advised to consult the publisher's version (publisher's PDF) if you wish to cite from it. Please check the document version below.

Document Version
Publisher's PDF, also known as Version of record

Publication date:
2013

[Link to publication in University of Groningen/UMCG research database](#)

Citation for published version (APA):

Nesterov, O., Matzen, S., Magen, C., Vlooswijk, A. H. G., Catalan, G., & Noheda, B. (2013). Thickness scaling of ferroelastic domains in PbTiO₃ films on DyScO₃. *Applied Physics Letters*, 103(14), 142901-1-142901-4. [142901]. <https://doi.org/10.1063/1.4823536>

Copyright

Other than for strictly personal use, it is not permitted to download or to forward/distribute the text or part of it without the consent of the author(s) and/or copyright holder(s), unless the work is under an open content license (like Creative Commons).

The publication may also be distributed here under the terms of Article 25fa of the Dutch Copyright Act, indicated by the "Taverne" license. More information can be found on the University of Groningen website: <https://www.rug.nl/library/open-access/self-archiving-pure/taverne-amendment>.

Take-down policy

If you believe that this document breaches copyright please contact us providing details, and we will remove access to the work immediately and investigate your claim.

Downloaded from the University of Groningen/UMCG research database (Pure): <http://www.rug.nl/research/portal>. For technical reasons the number of authors shown on this cover page is limited to 10 maximum.

Thickness scaling of ferroelastic domains in PbTiO₃ films on DyScO₃

O. Nesterov,¹ S. Matzen,¹ C. Magen,² A. H. G. Vlooswijk,¹ G. Catalan,³ and B. Noheda^{1,a)}

¹Zernike Institute for Advanced Materials, University of Groningen, 9747 AG Groningen, The Netherlands

²Laboratorio de Microscopías Avanzadas (LMA), Instituto de Nanociencia de Aragón (INA) - ARAID, and Departamento de Física de la Materia Condensada, 50018 Zaragoza, Spain

³CSIC, Ctr Invest. Nanoscience & Nanotechnology CIN2, Barcelona, Spain

(Received 5 July 2013; accepted 25 August 2013; published online 30 September 2013)

We report on the thickness dependence of the ferroelastic domains of PbTiO₃ films grown on (110)-DyScO₃ with low thicknesses (up to 240 nm), which fall outside the validity range of the square root law proposed by Roytburd. For slow-grown films, the data reveal the linear thickness dependence predicted by Pertsev and Zembilgotov, using a complete elastic description, while a 2/3 scaling exponent is found for fast-grown films. Extremely long domains running all through the samples have been observed in the latter case, compared to the short domains observed in slow-grown films. These differences are ascribed to the in-plane anisotropy for domain wall nucleation, which is likely caused by the anisotropic elastic modulus of the substrate. © 2013 AIP Publishing LLC.

[<http://dx.doi.org/10.1063/1.4823536>]

The response of domains and domain walls crucially affects (and often determines) the dielectric properties and switching behavior of ferroelectrics. This is particularly important in thin films where the ferroelectric (180°) and ferroelastic (non-180°) domain walls are formed in order to comply with the stringent electrical (large depolarizing field) and mechanical (substrate mismatch strain and clamping) boundary conditions.

The size of the domains increases with increasing film thickness as a result of the balance between the depolarizing field energy (for 180° domains)¹ or elastic strain energy (for non-180° domains)² and the domain wall formation energy. Thus, the thinner the films, the larger the domain wall density and the greater the influence of the walls on the ferroelectric properties. Moreover, domain walls break spatial symmetry and could add functionalities to the films when present in large amounts.³ It is therefore most relevant to have good control of the domain formation and the density of domain walls.⁴

Domain formation in ferroelectrics has been largely studied.^{2,3,5–15} In order to adapt to the substrate and to locally minimize the mismatch strain or the depolarizing field, the domains form in a periodic manner.^{6,7} It is known that there is a quadratic dependence, $W \propto d^{1/2}$, of the domain width (W) with the crystal thickness (d). In ferroelastic domains (typically 90° domains), this $d^{1/2}$ dependence is an approximation in the regime of $d \gg W$.² For smaller thicknesses, a linear dependence has been predicted by Pertsev and Zembilgotov (P&Z),⁸ but it has not been experimentally confirmed yet.

In this paper we investigate the thickness dependence of the periodicity of ferroelastic 90° domains (a/c twins) in the lower thickness regime using PbTiO₃ films grown on DyScO₃ substrates. This combination is chosen because there is a very small lattice mismatch between film and substrate at the growth temperature. This minimizes the formation of defects during growth. As the films are cooled down

strain develops and can be relaxed by forming a/c domains. The absence of defects allows these domains to form in a very periodic fashion.^{13,16} Interestingly, when the films are grown by pulsed laser deposition at high laser frequencies (10 Hz), extremely long domains are formed along one of the in-plane crystallographic directions, despite the very small difference in lattice parameters and thermal expansion coefficient of both in-plane lattice parameters of (110)-DyScO₃.

The thin films are grown on (110)-oriented DyScO₃ substrates¹⁷ by Pulsed Laser Deposition (PLD) from PbTiO₃ targets with 4 at. % excess lead. Orthorhombic (110)-DyScO₃ substrates are obtained from CrysTec GmbH. The two in-plane lattice directions are then [1-10] and [001], which we shall name a-axis and b-axis, respectively. The substrates exhibit double-terminated surfaces (with both DyO and ScO₂ surface layers), and they are chemically and thermally treated to get a single ScO₂ termination.¹⁸ This allows growing high quality SrRuO₃ layers since SrRuO₃ preferentially nucleates in that surface.¹⁹ An 8 nm-thick SrRuO₃ layer was grown between the film and the substrate. The SrRuO₃ layer is fully strained and acquires the lattice parameters of the substrate. The growth was monitored by Reflection High-Energy Electron Diffraction (RHEED). The RHEED intensity oscillations, together with x-ray reflectivity, are used to determine the thickness of the films. Two series of films have been grown at two different growth rates, using laser frequencies of 1 Hz and 10 Hz. The rest of the growth parameters were tuned to minimize the film roughness and maximize the RHEED intensity oscillations: the laser fluence, spot size at the target, substrate temperature, substrate-target distance, and O₂ pressure in the chamber were 1.5 J/cm², 0.8 mm², 570 °C, 48 mm, and 0.13 mbar, respectively, for the 1 Hz series, and 2.0 J/cm², 0.8 mm², 580 °C, 50 mm, and 0.06 mbar, respectively, for the 10 Hz series. These have resulted in deposition rates of about 1 unit cell per 55 s and 7 s. We will refer to these series as slow-grown and fast-grown, respectively. Scanning Transmission Electron Microscopy (STEM) experiments in High Angle Annular Dark Field (HAADF) were carried out in a probe-corrected

^{a)}Electronic mail: b.noheda@rug.nl

FEI Titan 60–300 microscope operated at 300 kV with a probe size of 1 Å. Atomic Force Microscopy (AFM) was performed using a VEECO (now Bruker) Dimension V microscope.

(110)-DyScO₃ does not have a totally squared in-plane lattice; however, the difference between the two in-plane parameters is typically considered too small to give rise to anisotropic domain formation. In agreement with this, for the slow-grown samples, we find domain walls along both in-plane directions. The domains organize in bundles with perpendicular domain walls forming four-fold symmetric patterns^{13,20} (see Fig. 1(a)). However, for the fast-grown samples, extremely long domain walls are observed along the *a*-axis of the substrate, as shown in Fig. 1(b), while shorter, less straight and less periodic domain walls are observed perpendicularly, along the *b*-axis. The length of the long domain walls ($\parallel a$) seems to mainly be limited by the length of the sample and only in rare cases a domain wall starts or ends at one of the perpendicular ($\parallel b$) walls. STEM reveals that despite the apparent differences between the sets of perpendicular walls in the AFM images of the fast-grown samples, both cross-sections consist of *a/c* twins (Figs. 1(c) and 1(d)).

In order to clarify the origin of the observed anisotropy, we have looked at the effect of the substrates terraces on the domain formation. PbTiO₃ thin films have been grown on DyScO₃ substrates with different direction of miscut, that is, different orientation of the substrate steps: forming 0°, 45°, and 90° with respect to the in-plane crystallographic directions. The domain structures created on two substrates with differently oriented terraces are shown in Figure 1S.²¹ It is observed that the long and straight domain walls form along the *a*-axis of (110)-DyScO₃, independent on the orientation of the substrate terraces.

Therefore, the long domain walls $\parallel a$ must form in response to the lattice strain experienced along the *b*-axis. At the growth temperature the misfit strain along the *a*-axis is close to zero (well below 0.1%) while the misfit strain along the *b*-axis is slightly tensile (0.12%) (see Figure 2S in Ref. 21).

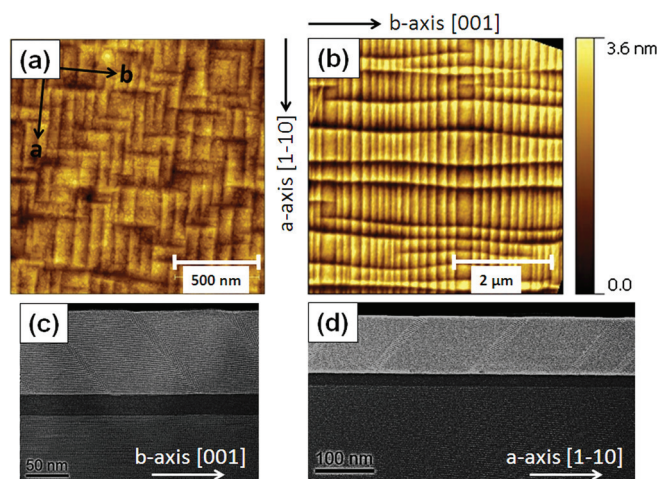


FIG. 1. (a) AFM images of a 100 nm thick slow-grown film and (b) a 200 nm fast-grown film. (c) Cross-sectional HAADF-STEM images of a 96 nm thick film in single-terminated (110)-DyScO₃ substrate in the (1-10) zone axis (cross-section parallel to the substrate *b*-axis) and (d) in the (001) zone axis (cross-section parallel to the substrate *a*-axis).

The difference between the fast-grown and slow-grown samples can be explained if we assume that the bulk phase transition is shifted upwards, already under such relative small strain values, such that the material grows in the ferroelectric phase.^{22,23} Then, differences in nucleation of the domain walls along both in-plane directions could explain the observed differences in domain formation. Because during fast growth the sample is far from thermodynamic equilibrium (higher supersaturation), if the energy barrier for nucleation of domain walls $\parallel b$ was larger than that of the walls $\parallel a$, the formation of the former walls would be hampered. Different energy barriers for domain wall nucleation can originate in the anisotropic elastic properties of DyScO₃ substrates, recently reported.²⁴ Slow-growth conditions will better reflect the equilibrium phase diagram of the system and its quite small misfit strain anisotropy.

That also implies that, during fast growth, the critical thickness for nucleation of domain walls would depend largely on the in-plane direction. This is, indeed, consistent with our observations: AFM pictures of PbTiO₃ films with different thicknesses are reproduced in Figure 2. It shows that for a given film, the density of walls $\parallel b$ is smaller than the density of walls $\parallel a$. In addition, while the walls $\parallel a$ are visible for thicknesses above 15 nm, the walls $\parallel b$ are only observed above 50 nm.

We now look at the thickness dependence of the domain periodicity. For too thin films, *a/c* domains are not expected; however, at these very small thicknesses the increased depolarizing field induces 180° domains.^{25,26} A crossover from 180° to 90° domains is thus expected at a particular thickness. In this case the crossover between 180° and 90° domains is found at $d \sim 10$ nm but only for $d > 15$ nm, we are able to observe well-defined, ordered *a/c* domains.^{23,27} Figure 2 shows the high degree of ordering of the *a/c* domains (with walls $\parallel a$) in PbTiO₃ on DyScO₃, and the robustness of the domain size across the film allows us to monitor their size not only by local probe techniques, such as AFM and piezo-AFM, but also by x-ray diffraction (XRD).^{13,20} Typically, the best sensitivity is obtained using XRD for the relatively thinner films (Fig. 2(a)) and using AFM for the thicker films (Figs. 2(b) and 2(c)).

The data collected for all the samples, including slow-grown and fast-grown samples, are summarized in Figure 3, showing the domain period (*W*) as a function of the film thickness (*d*) in a double logarithmic scale. The slow-grown films follow the trend predicted by P&Z:⁸ a minimum introducing a change of trend at the lowest thicknesses and a linear *W*(*d*) dependence for thickness $30 \text{ nm} < d < 100 \text{ nm}$. A quantitative fit was not successful, and the best possible fit (using $T = 440^\circ \text{C}$ and $\sigma = 19 \text{ mJ/m}^2$) was off by 41 nm (see Figure 3 and 3S in Ref. 21). For the fast-grown samples, the experimental domain size does not follow the predicted evolution, since it does scale neither as $d^{1/2}$ (Ref. 2) nor linearly with *d*.⁸ Instead, fitting the data in Figure 3 for the fast-grown samples results in an exponent $n = 0.68 \pm 0.03$ ($n \approx 2/3$). Our experimental results exhibit thus a behavior in between the classic Roytburd's square-root law and Pertsev's linear law. One possible explanation is that we are probing the crossover between these two regimes. One can argue that, indeed, for the lowest thicknesses ($d < 40 \text{ nm}$) the data are not inconsistent with a

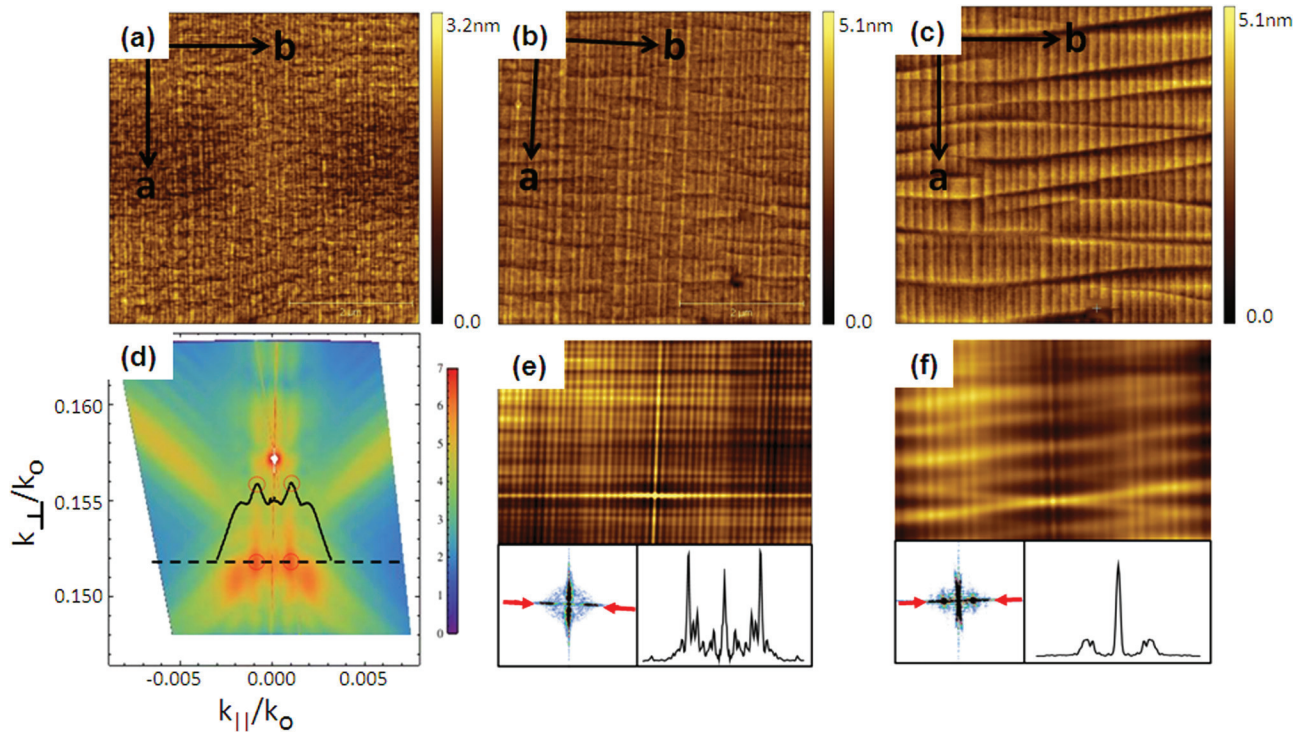


FIG. 2. The top panels show AFM images ($5 \mu\text{m} \times 5 \mu\text{m}$) of PbTiO₃ layers on DyScO₃ with different thicknesses, d , and average domain periods, W : (a) $d = 50$ nm, $W = 80$ nm; (b) $d = 80$ nm, $W = 105$ nm; (c) $d = 180$ nm, $W = 197$ nm. The substrate b-axis is horizontal in all three images. The method used to determine the domain size is shown for each sample in the bottom panels: (d) x-ray reciprocal space mapping around the (002)_{pc} reflection shows the intensity oscillations due to periodic domains. Axes are in units of $k_0 = 2\pi/\lambda$, being λ the x-ray wavelength. The color scale represents $\log(I)$. A linear scan along the dashed line (rocking curve) is plotted as a solid curve showing the intensity maxima from whose $k_{||}$ values the domain periodicity is obtained; (e) and (f) AFM auto-correlation images of (b) and (c), respectively, and their Fast Fourier Transforms (in the insets).

$n = 1$ exponent; however, for the large thickness regime, there is no indication of approaching $n = 1/2$. Intermediate scaling exponents $1/2 < n < 1$ have been reported before for fractal domains,²⁸ but clearly the wall roughening mechanism cannot be invoked here, since our domains are perfectly smooth.

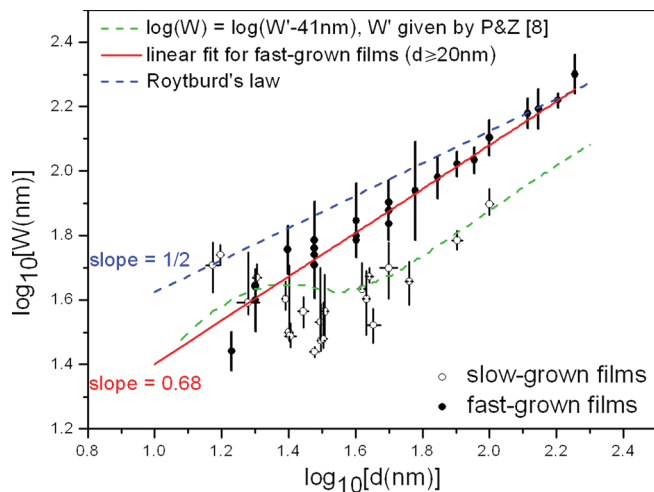


FIG. 3. Log-log plot of the observed domain period, W , as a function of film thickness, d , for 90° domains in PbTiO₃ thin films grown on SrRuO₃-buffered DyScO₃ substrates. The data for the slow-grown and fast-grown samples are plotted as open and close circles, respectively. The red line is a linear fit for the fast-grown films with $d \geq 20$ nm. The dashed blue line corresponds to the $n = 1/2$ exponent² and uses the materials parameters at $T = 480^\circ\text{C}$ and a domain wall energy of 21 mJ/m^2 . The dashed green line is obtained subtracting 41 nm from the domain period produced with the P&Z model⁸ using the lattice parameters at 440°C and a domain wall energy $\sigma = 19 \text{ mJ/m}^2$ (see Ref. 21).

Fractional scaling exponents have also been extracted from switching dynamics,²⁹ and thus it may be the case that our exponent reflects the dynamics of domain nucleation.³⁰ Indeed, it rather looks like we are seeing a law that differs from that predicted by equilibrium models, something unsurprising for such fast-grown films.

According to the usual description of the energy balance between domains and domain walls,¹² the domain size is found by minimizing the sum of the elastic energy stored within the domains plus the energy of the domain walls. This minimization leads to the well-known Kittel formula, $W = \sqrt{\frac{\sigma}{U}d}$, where U is the volume energy density of the domains and σ the energy per unit area of the walls. In the standard derivation of Kittel's law it is assumed that U and σ are independent of the thickness d , but this is not a realistic assumption for very thin films, where strain is only partially relaxed or when structural and compositional gradients,³¹ as well as competing relaxation mechanisms with different critical thicknesses (such as dislocations and twinning), introduce a thickness dependence on the energy densities. Within the thickness range of this study, the domain size scales as a power law, which implies that the energy densities can also be expressed as power laws: $U = \eta d^K$ and $\sigma = \eta d^L$ and Kittel's law thus becomes $W = \sqrt{\eta/\eta d^{(-K+L+1)/2}}$. Comparing with the experimental result, $W \propto d^{2/3}$, we get that $L-K = 1/3$.

The exponent K that determines the volume energy density as a function of thickness has been amply studied by the semiconductor thin film community. The equilibrium models for strain relaxation and formation of dislocations^{32–34} give rise to a residual strain that is inversely proportional to the

layer thickness ($\varepsilon \propto d^{-1}$), which, given that elastic energy is proportional to the square of the strain (Hooke's law), implies that $K = -2$. On the other hand, it has also been shown that during epitaxial growth, the non-equilibrium kinetics of dislocation formation can lead to $\varepsilon \propto d^{-1/2}$ (or $U \propto d^{-1}$).³⁵ In contrast, much less is known about the value of L that determines the thickness dependence of the domain wall energy. Since the energy cost of the walls is proportional to the spontaneous strain in the domains, a thickness dependence of the residual strain must also result in a thickness dependence of the domain wall energy. If we accept $-2 < K < -1$ as the two limiting cases for the volume energy density, then compliance with our empirical results requires $-5/3 < L < -2/3$ for the equilibrium and non-equilibrium growth scenarios, respectively.

To conclude, we investigate the thickness scaling of the domain periodicity of slow-grown and fast-grown samples. We show that, for films grown on (110)-DyScO₃, working out of equilibrium with well-defined conditions allows a large degree of control of the domain width and morphology, beyond the predictions of thermodynamical models. This is enabled by the differences in domain wall nucleation along different crystal in-plane directions, which is most likely caused by the anisotropy in the elastic modulus of the substrate. Note: After acceptance of this paper, we have learned of unpublished work by L. Feigl and co-workers at EPFL-Lausanne, showing an even stronger anisotropy on PbZr_{0.1}Ti_{0.90}O₃ films grown on DyScO₃ (paper presented at the IMF13-Krakow September 2013).

This work was supported by NanoNextNL, a micro and nanotechnology consortium of the Government of the Netherlands and 130 partners.

¹C. Kittel, *Phys. Rev.* **70**, 965 (1946).

²A. L. Roytburd, *Phys. Status Solidi A* **37**, 329 (1976).

³E. Salje and H. L. Zhang, *Phase Transitions* **82**, 452 (2009).

⁴G. Catalan, J. Seidel, R. Ramesh, and J. F. Scott, *Rev. Mod. Phys.* **84**, 119 (2012).

⁵T. Mitsui and J. Furuichi, *Phys. Rev.* **90**, 193 (1953).

⁶B. S. Kwak, A. Erbil, B. J. Wilkens, J. D. Budai, M. F. Chisholm, and L. A. Boatner, *Phys. Rev. Lett.* **68**, 3733 (1992).

⁷W. Pompe, X. Gong, Z. Suo, and J. S. Speck, *J. Appl. Phys.* **74**, 6012 (1993); J. S. Speck and W. Pompe, *J. Appl. Phys.* **76**, 466 (1994).

⁸N. A. Pertsev and A. G. Zembilgotov, *J. Appl. Phys.* **78**, 6170 (1995).

⁹S. Stemmer, S. K. Streiffer, F. Ernst, M. Rhle, W.-Y. Hsu, and R. Raj, *Solid State Ionics* **75**, 43 (1995).

¹⁰B. Meyer and D. Vanderbilt, *Phys. Rev. B* **63**, 205426 (2001).

¹¹S. K. Streiffer, J. A. Eastman, D. D. Fong, C. Thompson, A. Munkholm, M. V. R. Murty, O. Auciello, G. R. Bai, and G. B. Stephenson, *Phys. Rev. Lett.* **89**, 067601 (2002); D. D. Fong, G. B. Stephenson, S. K. Streiffer, J. A. Eastman, O. Auciello, P. H. Fuoss, and C. Thompson, *Science* **304**, 1650 (2004).

¹²A. Schilling, T. B. Adams, R. M. Bowman, J. M. Gregg, G. Catalan, and J. F. Scott, *Phys. Rev. B* **74**, 024115 (2006).

¹³A. H. G. Vlooswijk, B. Noheda, G. Catalan, A. Janssens, B. Barcones, G. Rijnders, D. H. A. Blank, S. Venkatesan, B. Kooi, and J. T. M. de Hosson, *Appl. Phys. Lett.* **91**(11), 112901 (2007).

¹⁴R. Ramesh and D. G. Schlom, *MRS Bull.* **33**, 1006 (2008).

¹⁵A. K. Tagantsev, L. E. Cross, and J. Fousek, *Domains in Ferroic Crystals and Thin Films* (Springer, 2010).

¹⁶S. Venkatesan, A. Vlooswijk, B. J. Kooi, A. Morelli, G. Palasantzas, J. T. M. De Hosson, and B. Noheda, *Phys. Rev. B* **78**, 104112 (2008).

¹⁷M. D. Biegalski, J. H. Haeni, S. Trolier-McKinstry, D. G. Schlom, C. D. Brande, and A. J. Ven Graitis, *J. Mater. Res.* **20**, 952 (2005).

¹⁸J. E. Kleibeuker, G. Koster, W. Siemons, D. Dubbink, B. Kuiper, J. L. Blok, C. H. Yang, J. Ravichandran, R. Ramesh, J. E. ten Elshof *et al.*, *Adv. Funct. Mater.* **20**, 3490 (2010).

¹⁹R. Egoavil, H. Tan, J. Verbeeck, S. Bals, B. Smith, B. Kuiper, G. Rijnders, G. Koster, and G. Van Tendeloo, *Appl. Phys. Lett.* **102**, 223106 (2013).

²⁰G. Catalan, A. Lubk, A. H. G. Vlooswijk, E. Snoeck, C. Magen, A. Janssens, G. Rispens, G. Rijnders, D. H. A. Blank, and B. Noheda, *Nature Mater.* **10**, 963 (2011).

²¹See supplementary material at <http://dx.doi.org/10.1063/1.4823536> for AFM images on miscut orientation dependence, lattice parameters as a function of temperature, and further details on the fits with the P&Z model.

²²V. G. Koukhar, N. A. Pertsev, and R. Waser, *Appl. Phys. Lett.* **78**, 530 (2001).

²³Q. Y. Qiu, V. Nagarajan, S. P. Alpay, *Phys. Rev. B* **78**, 064117 (2008).

²⁴M. Janovska, P. Sedlak, H. Seiner, M. Landa, P. Marton, P. Ondrejovic, and J. Hlinka, *J. Phys.: Condens. Matter* **24**, 385404 (2012).

²⁵J. Junquera and P. Ghosez, *Nature* **422**, 506 (2003).

²⁶I. Kornev, H. Fu, and L. Bellaiche, *Phys. Rev. Lett.* **93**, 196104 (2004).

²⁷A. H. G. Vlooswijk, "Structure and domain formation in ferroelectric thin films," Ph.D. thesis (Zernike Institute for Advanced Materials, Groningen, 2009).

²⁸G. Catalan, H. Bea, S. Fusil, M. Bibes, P. Paruch, A. Barthelemy, and J. F. Scott, *Phys. Rev. Lett.* **100**, 027602 (2008).

²⁹J. F. Scott and C. A. Paz de Araujo, *Science* **246**, 1400 (1989).

³⁰P. Paruch, A. B. Kolton, X. Hong, C. H. Ahn, and T. Giamarchi, *Phys. Rev. B* **85**, 214115 (2012).

³¹G. Catalan, B. Noheda, J. McAneney, L. J. Sinnamon, and J. M. Gregg, *Phys. Rev. B* **72**, 020102 (2005).

³²J. W. Matthews and A. E. Blakeslee, *J. Cryst. Growth* **27**, 118 (1974).

³³R. People and J. C. Bean, *Appl. Phys. Lett.* **47**, 322 (1985).

³⁴G. Sheng, J. M. Hu, J. X. Zhang, Y. L. Li, Z. K. Liu, and L. Q. Chen, *Acta Mater.* **60**, 3296 (2012).

³⁵A. V. Drigo, A. Aydinli, A. Carnera, F. Genova, C. Rigo, C. Ferrari, P. Franzosi, and G. Salvati, *J. Appl. Phys.* **66**, 1975 (1989).